Heathcock L, Jenkins R, Schultz CJ, Gilbert MR, Group RTO (2011) RTOG 0525: Molecular correlates from a randomized phase III trial of newly diagnosed glioblastoma. ASCO Annu Meet Proc 29(18_suppl):LBA2000

21. Wick A, Felsberg J, Steinbach JP, Herrlinger U, Platten M, Blaschke B, Meyermann R, Reifenberger G, Weller M, Wick W (2007) Efficacy and tolerability of temozolomide in an alternating weekly regimen in patients with recurrent glioma. J Clin Oncol 25(22):3357–3361. doi:10.1200/JCO.2007.10.7722
22. Quinn JA, Jiang SX, Reardon DA, Desjardins A, Vredenburgh JJ, Rich JN, Gururangan S, Friedman AH, Bigner DD, Sampson JH, McLendon RE, Herndon JE 2nd, Walker A, Friedman HS (2009) Phase II trial of temozolomide plus O^6-benzylguanine in adults with recurrent, temozolomide-resistant malignant glioma. J Clin Oncol 27(8):1262–1267. doi:10.1200/JCO.2008.18.8417
23. Quinn JA, Pluda J, Dolan ME, Delaney S, Kaplan R, Rich JN, Friedman AH, Reardon DA, Sampson JH, Colvin OM, Haglund MM, Pegg AE, Moschel RC, McLendon RE, Provenzale JM, Gururangan S, Tourt-Uhlig S, Herndon JE 2nd, Bigner DD, Friedman HS (2002) Phase II trial of carmustine plus O(6)-benzylguanine for patients with nitrosourea-resistant recurrent or progressive malignant glioma. J Clin Oncol 20(9):2277–2283
24. Stupp R, Mason WP, van den Bent MJ, Weller M, Fisher B, Taphoorn MJ, Belanger K, Brandes AA, Marosi C, Bogdahn U, Curschmann J, Janzer RC, Ludwin SK, Gorlia T, Allgeier A, Lacombe D, Cairncross JG, Eisenhauer E, Mirimanoff RO (2005) Radiotherapy plus concomitant and adjuvant temozolomide for glioblastoma. N Engl J Med 352(10):987–996
25. Brandes AA, Tosoni A, Spagnolli F, Frezza G, Leonardi M, Calbucci F, Franceschi E (2008) Disease progression or pseudoprogression after concomitant radiochemotherapy treatment: pitfalls in neurooncology. Neuro Oncol 10(3):361–367. doi:10.1215/15228517-2008-008
26. van den Bent MJ (2010) Interobserver variation of the histopathological diagnosis in clinical trials on glioma: a clinician's perspective. Acta Neuropathol 120(3):297–304. doi:10.1007/s00401-010-0725-7
27. Hildebrand J, Gorlia T, Kros JM, Afra D, Frenay M, Omuro A, Stupp R, Lacombe D, Allgeier A, van den Bent MJ (2008) Adjuvant dibromodulcitol and BCNU chemotherapy in anaplastic astrocytoma: results of a randomised European Organisation for Research and Treatment of Cancer phase III study (EORTC study 26882). Eur J Cancer 44(9):1210–1216. doi:10.1016/j.ejca.2007.12.005
28. Coons SW, Johnson PC, Scheithauer BW, Yates AJ, Pearl DK (1997) Improving diagnostic accuracy and interobserver concordance in the classification and grading of primary gliomas. Cancer 79(7):1381–1393

Int Canc Conf J (2012) 1:53–57
DOI 10.1007/s13691-011-0009-7

CASE REPORT

Reactivation of cytomegalovirus following treatment of malignant glioma with temozolomide

Yoshiko Okita · Yoshitaka Narita · Yasuji Miyakita · Makoto Ohno · Kohki Aihara · Shinichiro Mori · Takamasa Kayama · Soichiro Shibui

Received: 2 September 2011 / Accepted: 14 November 2011 / Published online: 20 December 2011

Abstract Temozolomide is a standard chemotherapeutic agent in the treatment of malignant gliomas. Lymphocytopenia is reported to be the most frequent and severe adverse effect, which causes opportunistic infections such as pneumocystis pneumonia (PCP) and increases the risk of the reactivation of viruses such as hepatitis B virus (HBV) and cytomegalovirus (CMV). However, the incidence of temozolomide-induced CMV reactivation remains unclear. We report on a case of a 62-year-old female with gliomatosis cerebri who had severe lymphocytopenia and pneumonia following concurrent temozolomide treatment and prophylaxis for PCP. She presented cough, fever, and severe lymphocytopenia 1 month after chemoradiotherapy with temozolomide. Her serum β-D-glucan levels remained within the normal range, which was helpful to rule out a diagnosis of PCP. Other opportunistic infections were ruled out, and a blood test for the CMV antigen was positive for pp65 antigenemia. The patient was diagnosed as having CMV pneumonia. She was treated with ganciclovir and recovered. It was very difficult to distinguish between PCP and CMV pneumonia with only the clinical presentation and radiological findings. When a patient receives temozolomide, it is important to be aware of the potential for a CMV reactivation. The serum β-D-glucan levels and pp65 antigenemia are very useful for diagnosis of CMV pneumonia.

Y. Okita · Y. Narita (✉) · Y. Miyakita · M. Ohno · K. Aihara · T. Kayama · S. Shibui
Department of Neurosurgery and Neuro-Oncology, National Cancer Center Hospital, 5-1-1 Tsukiji, Chuo-ku, Tokyo 104-0045, Japan
e-mail: yonarita@ncc.go.jp

S. Mori
Department of Stem Cell Transplantation, National Cancer Center Hospital, Tokyo, Japan

Keywords Cytomegalovirus · Reactivation · Temozolomide · Immunosuppression · Malignant glioma

Introduction

Temozolomide is the standard therapy for patients with malignant glioma [1]. The incidence of severe adverse events, such as leukopenia, anemia, and thrombocytopenia, as well as vomiting or nausea, has been reported to be rather low and reversible, compared with other chemotherapeutic agents previously used for malignant gliomas [2]. However, severe lymphocytopenia induced by temozolomide causes opportunistic infections, such as pneumocystis pneumonia (PCP) [3, 4] or fulminant hepatitis due to the reactivation of the HBV [5]. Temozolomide has also been reported to induce CMV reactivation [4, 6–9], which is due to lymphocytopenia, and to cause CMV pneumonia [6–8], colitis [4, 7, 9], and transverse myelitis [4].

We herein report on the case of a patient with severe lymphocytopenia and CMV pneumonia following temozolomide treatment.

Case report

A 62-year-old woman with gliomatosis cerebri was admitted with pneumonia. Initially, she presented with dementia and scored 20 points on the Mini-Mental State Examination. She was diagnosed with gliomatosis cerebri in both frontal to left temporoparietal lobes on the basis of magnetic resonance (MR) images (Fig. 1a). The tumor was biopsied from the left frontal lobe, and the pathological diagnosis was diffuse astrocytoma, grade 2. She was treated with temozolomide alone because the irradiation field

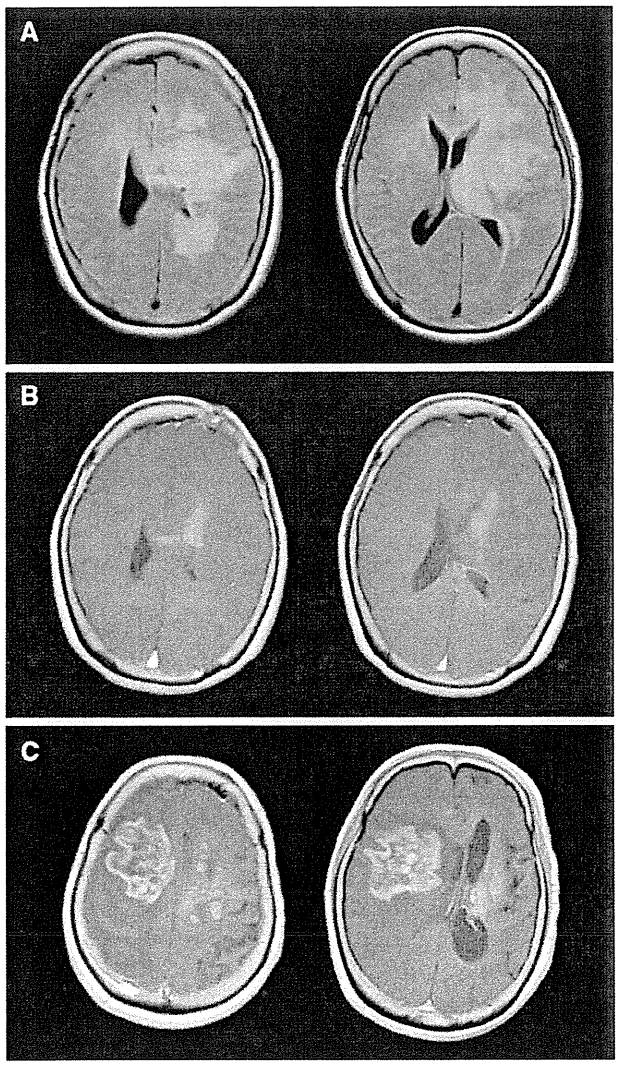

Fig. 1 **a** Preoperative MR images: tumor in the bilateral frontal to left temporoparietal lobes in the fluid-attenuated inversion recovery (FLAIR) image. **b** MR images of first recurrence: newly enhanced lesion in the bilateral frontal lobes involving the corpus callosum. **c** MR images of second recurrence: newly developed ring-enhancing lesions with tumor recurrence in the bilateral frontal lobes

was very large and extended from the left dominant hemisphere to the right frontal lobe and because there was a possibility of radiation-induced cognitive dysfunction. She underwent chemotherapy with temozolomide (150 mg/m^2 per day) for the first 5 days of a 28-day cycle, and continued temozolomide treatment (200 mg/m^2) almost every 4 weeks. After 6 cycles of temozolomide, she presented with global aphasia and the inability to walk. MR imaging showed a mass that was slightly enhanced with gadolinium diethylenetriamine pentaacetic acid in the left frontal lobe that was not seen before the initial treatment (Fig. 1b). She was diagnosed with recurrence and malignant change from grade 2 astrocytoma, and she underwent and completed radiotherapy (54 Gy in 30 fractions) and concurrent temozolomide (75 mg/m^2 per day) treatment for 42 days. She was given 20 mg/day predonisolone, and her neurological symptoms recovered slightly. At the same time, she took cotrimoxazole (trimethoprim–sulfamethoxazole 1 g/day) for prophylaxis against PCP. Before chemoradiation therapy was started, her white blood cell (WBC) count, absolute neutrophil count (ANC), and absolute lymphocyte count (ALC) were 6,300 cells/μL, 5,390 neutrophils/μL, and 570 lymphocytes/μL, respectively. In addition, the Common Terminology Criteria for Adverse Events v4.0 (CTCAE) for grade 2 lymphocytopenia related to TMZ were observed. After the chemoradiation therapy, the lymphocytopenia worsened to grade 4 (WBC count 2,300 cells/μL, ANC 2,160 neutrophils/μL, and ALC 80 lymphocytes/μL), and she was discharged without any respiratory symptoms and was followed up with predonisolone (20 mg/day). She continued to take cotrimoxazole for prophylaxis. Total administered dose of TMZ after chemoradiation therapy was 12,800 mg. Two weeks after completion of the chemoradiation therapy, her ALC recovered slightly (220 lymphocytes/μL), but the grade 3 lymphocytopenia persisted. One month after the completion of the radiotherapy and temozolomide treatment, she experienced cough, fever, and dyspnea, and she was readmitted to our hospital.

At admission, her WBC count, ANC, and ALC were 4,500/μL, 4,370/μL, and 0/μL, respectively, and grade 4 lymphocytopenia was observed. Radiography (Fig. 2b) and a high-resolution computed tomography (CT) scan of the chest (Fig. 2c) were performed, which revealed interstitial pneumonitis with diffuse bilateral interstitial infiltrations. After consulting the chief of the infection control team (ICT), she was treated with the antibiotics cefazolin (CEZ) and azithromycin (AZM). The serum β-D-glucan levels remained within the normal range (8.3 pg/mL). We checked sputum and blood culture, the influenza virus antigen, the urinary antigen of *Legionella*, and screened for the Epstein–Barr virus, but those examinations were negative for the cause of pneumonia. Because the patient took cotrimoxazole as prophylaxis for PCP during and after chemoradiation therapy, CMV pneumonia was highly suspected (Fig. 3). A blood sample was obtained in order to test for the CMV antigen, and it was positive for pp65 antigenemia (329 cells per 43,000 leukocytes). It was difficult to diagnose PCP or CMV pneumonia on the basis of the CT radiological findings. She was diagnosed as having CMV pneumonia because other opportunistic infections were ruled out, and the blood test for the CMV antigen was positive for pp65 antigenemia. She started to receive ganciclovir together with antibiotics including CEZ, AZM, and cefmetazole (CMZ), and the predonisolone was gradually tapered. The intravenous ganciclovir dosage was 5 mg/kg

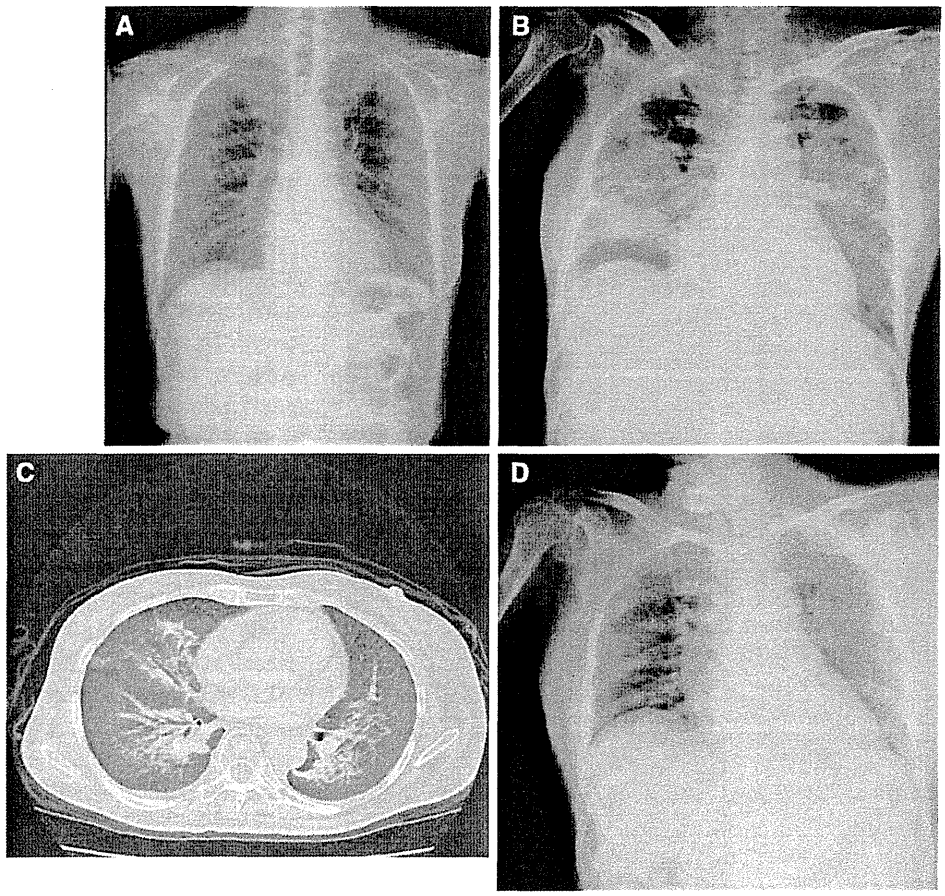

Fig. 2 **a** Chest radiograph before biopsy on first admission. **b** Pretreatment chest radiograph. **c** Pretreatment chest CT; interstitial pneumonitis with diffuse bilateral interstitial infiltrates was verified. **d** Post-treatment chest radiograph showing improvement of interstitial pneumonitis

twice a day for 14 days. Furthermore, the frequency of intravenous ganciclovir was decreased once a day for next 12 days. She became afebrile about 1 week after the treatment with ganciclovir. After receiving ganciclovir for 20 days and antibiotics for 23 days, the test for the CMV pp65 antigen was negative and her respiratory state recovered gradually (Fig. 2d). Five months after completion of the chemoradiation therapy, MR imaging showed tumor progression (Fig. 1c), and she became bedridden. She was eventually transferred to another hospital for palliative treatment of her malignant disease.

Discussion

Temozolomide is the standard therapy for patients with malignant glioma [1]. The total incidence and incidence of grade 3/4 leukopenia were 38 and 3%, those of neutropenia were 47 and 6%, those of lymphocytopenia were 50 and 25%, and those of thrombocytopenia were 31 and 9% in another clinical study conducted in Japan [10]. At our institution, grade 3/4 lymphocytopenia occurred in 40% of the patients just after radiotherapy with concurrent temozolomide treatment and in 20% of the patients after 6 cycles of adjuvant temozolomide chemotherapy (data not shown). Because temozolomide is associated with $CD4^+$ T-cell dysfunction, treatment with temozolomide is possibly associated with a decline of the immune system and an increased susceptibility to opportunistic infections such as PCP [3, 4]. This characteristic immunosuppression also induces CMV reactivation as a rare complication [4, 6–9]. The incidence and risk factors of temozolomide-induced CMV reactivation, as well as its optimal management, remain unclear. Steroids also causes immunosuppression and the majority of reported cases of opportunistic CMV infection occurred when patients were treated concurrently with temozolomide and steroids [4, 6–9], including our case. Therefore, treatment with temozolomide in combination with steroids is supposed to be the cause of immunosuppression and subsequent CMV reactivation.

It was reported that 2.9% of adults with leukemia were diagnosed with CMV pneumonia [11]. CMV reactivation due to severe lymphocytopenia has been reported to occur in only 0.3% of patients with solid tumors such as lung and breast cancers who received docetaxel-based chemotherapy [12]. The risk of infection is increased with the use of T-lymphocytotoxic chemotherapies, e.g., cytarabine, fludarabine, or high-dose cyclophosphamide and

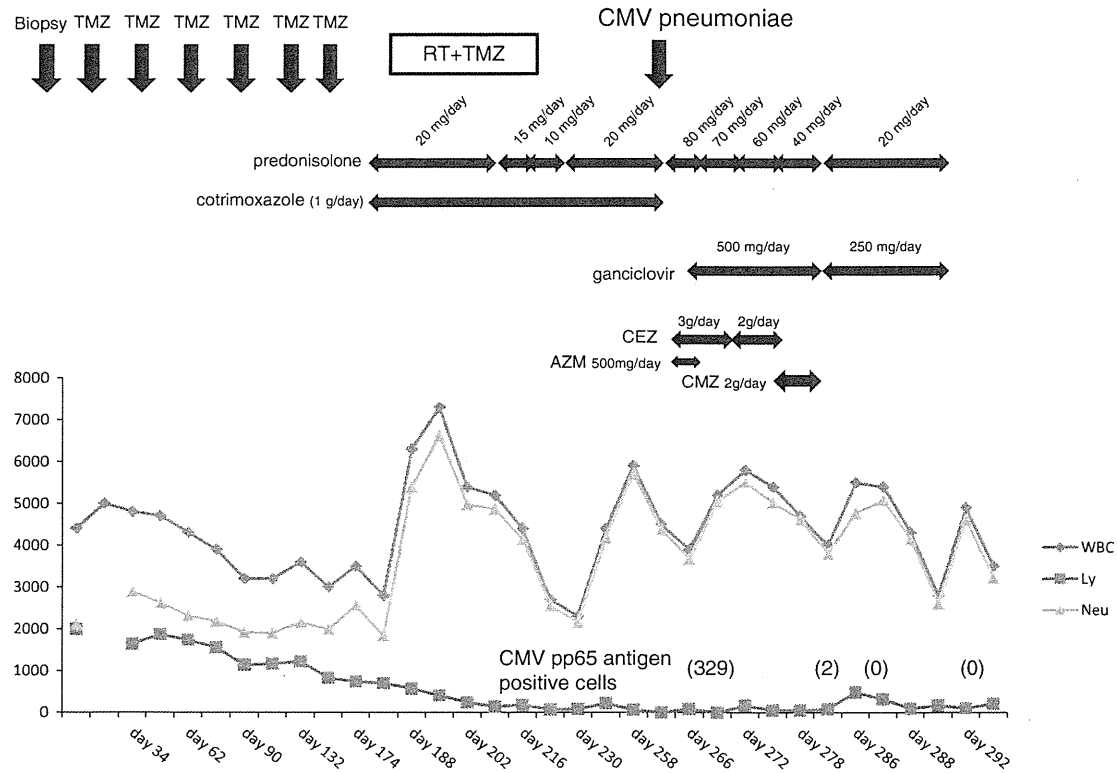

Fig. 3 Clinical course of malignant glioma patient with CMV pneumoniae. Biopsy was performed at day 0. *RT* radiation therapy, *TMZ* temozolomide, *WBC* white blood cell, *Ly* lymphocyte, *Neu* neutrophil, *CEZ* cefazolin, *AZM* azithromycin, *CMZ* cefmetazole

with the use of T-cell suppressors, e.g., methotrexate or corticosteroids [13].

The clinical presentation of both PCP and CMV pneumonia consists of fever, dyspnea, and unproductive cough and the radiological differentiation of CMV pneumonia and PCP is usually difficult even by thin-section CT scans [14–16]. Prophylaxis for PCP with cotrimoxazole has been recommended since the first research studies were performed with temozolomide [17]. According to Green et al. [18], prophylactic cotrimoxazole was highly effective in preventing PCP infection, and the treatment lowered the incidence of PCP infection by 91%. Even when grade 3/4 lymphocytopenia is observed, it seems that patients treated with temozolomide and prophylactic cotrimoxazole are at low risk of developing PCP. At our institution, patients receiving more than 15 mg/day of predonisolone or those with grade 3/4 lymphocytopenia received cotrimoxazole (1 g/day) as prophylaxis for PCP. Previously, three cases of CMV pneumonia that were induced by temozolomide were reported, and lymphocytopenia occurred in all of them [6–8]. Two of them experienced only CMV pneumonia, and prophylaxis for PCP with cotrimoxazole had been provided for one of them [7], whereas cotrimoxazole was not mentioned for the other case [6]. The third case reported by Douzinas et al. [8] was not offered cotrimoxazole and developed severe PCP and coexisting CMV pneumonia. Furthermore, Vogel et al. [16] reported that 84% of patients who were diagnosed with CMV pneumonia had received PCP prophylaxis. However, none of the patients who were diagnosed with PCP received PCP prophylaxis.

In previous reports, screening for a CMV infection by means of antigenemia or CMV polymerase chain reaction assays was carried out, and these methods correlated with disease identification [6–9]. Tasaka et al. [19] reported that serum β-D-glucan levels were significantly higher in PCP-positive patients than in PCP-negative patients ($p < 0.0001$). They showed that the sensitivity, specificity, and negative predictive value of β-D-glucan levels were 92.3, 86.1, and 98.0%, respectively, and the cutoff level of β-D-glucan was estimated to be 31.1 pg/mL [19]. Other reports describing temozolomide-induced CMV pneumonia so far have not reported the levels of β-D-glucan [4, 6–9]. Normal serum β-D-glucan level and pp65 antigenemia were very useful for diagnosis of CMV pneumonia in our case.

According to a report in 1973 [20], the rate of CMV antibody carriers in Japan was 96% and those in Asia and Africa were 90–100%, both higher than that in Western countries (40–50%). The rate of CMV antibody carriers among pregnant women in Japan decreased gradually from 93.2% in 1980 to 66.7% in 1995 [21] but it is still high. It is

important to be aware of the potential for CMV reactivation during treatment with temozolomide and steroids, particularly in Asian and African countries.

Acknowledgments Dr. Okita receives research support from Grant-in-Aid for Scientific Research from the Ministry of Education, Culture, Sports, Science and Technology (MEXT). Dr. Narita receives research support from Health Labour Sciences Research Grant and National Cancer Center Research and Development Fund. Dr. Kayama receives research support from Grant-in-Aid for Scientific Research from the Ministry of Education, Culture, Sports, Science and Technology (MEXT), Health Labour Sciences Research Grant and National Cancer Center Research and Development Fund. Dr. Shibui receives research support from Health Labour Sciences Research Grant and National Cancer Center Research and Development Fund.

Conflict of interest We declare that there are no conflict of interest.

References

1. Stupp R, Mason WP, van den Bent MJ et al (2005) Radiotherapy plus concomitant and adjuvant temozolomide for glioblastoma. N Engl J Med 352:987–996
2. Dario A, Tomei G (2006) The safety of the temozolomide in patients with malignant glioma. Curr Drug Saf 1:205–222
3. Yu SK, Chalmers AJ (2007) Patients receiving standard-dose temozolomide therapy are at risk of *Pneumocystis carinii* pneumonia. Clin Oncol (R Coll Radiol) 19:631–632
4. Schwarzberg AB, Stover EH, Sengupta T et al (2007) Selective lymphopenia and opportunistic infections in neuroendocrine tumor patients receiving temozolomide. Cancer Invest 25:249–255
5. Ohno M, Narita Y, Miyakita Y et al (2011) Reactivation of hepatitis B virus after glioblastoma treatment with temozolomide. Neurol Med Chir (Tokyo) 51:728–731
6. Yaman E, Coskun U, Ozturk B et al (2009) Opportunistic cytomegalovirus infection in a patient receiving temozolomide for treatment of malignant glioma. J Clin Neurosci 16:591–592
7. Meije Y, Lizasoain M, Garcia-Reyne A et al (2010) Emergence of cytomegalovirus disease in patients receiving temozolomide: report of two cases and literature review. Clin Infect Dis 50: e73–e76
8. Douzinas EE, Flevari K, Andrianakis I et al (2010) Oral atovaquone for the treatment of severe *Pneumocystis jirovecii* pneumonia in a patient with glucose-6-phosphate dehydrogenase deficiency. Scand J Infect Dis 42:76–78
9. De Jesus A, Grossman SA, Paun O (2009) Cytomegalovirus associated colonic pseudotumor: a consequence of iatrogenic immunosuppression in a patient with primary brain tumor receiving radiation and temozolomide. J Neurooncol 94:445–448
10. Nishikawa R, Shibui S, Maruno M et al (2006) Efficacy and safety of monotherapy with temozolomide in patients with anaplastic astrocytoma at first relapse–a phase II clinical study. Gan To Kagaku Ryoho 33:1279–1285
11. Nguyen Q, Estey E, Raad I et al (2001) Cytomegalovirus pneumonia in adults with leukemia: an emerging problem. Clin Infect Dis 32:539–545
12. Souglakos J, Kotsakis A, Kouroussis C et al (2002) Nonneutropenic febrile episodes associated with docetaxel-based chemotherapy in patients with solid tumors. Cancer 95:1326–1333
13. Vento S, Cainelli F, Temesgen Z (2008) Lung infections after cancer chemotherapy. Lancet Oncol 9:982–992
14. McGuinness G, Gruden JF (1999) Viral and *Pneumocystis carinii* infections of the lung in the immunocompromised host. J Thorac Imaging 14:25–36
15. Raoof S, Naidich DP (2004) Imaging of unusual diffuse lung diseases. Curr Opin Pulm Med 10:383–389
16. Vogel MN, Brodoefel H, Hierl T et al (2007) Differences and similarities of cytomegalovirus and pneumocystis pneumonia in HIV-negative immunocompromised patients thin section CT morphology in the early phase of the disease. Br J Radiol 80: 516–523
17. Stupp R, Dietrich PY, Ostermann Kraljevic S et al (2002) Promising survival for patients with newly diagnosed glioblastoma multiforme treated with concomitant radiation plus temozolomide followed by adjuvant temozolomide. J Clin Oncol 20:1375–1382
18. Green H, Paul M, Vidal L et al (2007) Prophylaxis of pneumocystis pneumonia in immunocompromised non-HIV-infected patients: systematic review and meta-analysis of randomized controlled trials. Mayo Clin Proc 82:1052–1059
19. Tasaka S, Hasegawa N, Kobayashi S et al (2007) Serum indicators for the diagnosis of pneumocystis pneumonia. Chest 131: 1173–1180
20. Krech U (1973) Complement-fixing antibodies against cytomegalovirus in different parts of the world. Bull World Health Organ 49:103–106
21. Hoshiba T, Asamoto A, Yabuki Y (1998) Decreasing seropositivity of cytomegalovirus of pregnant women in Japan. Nippon Rinsho 56:193–196

Neurol Med Chir (Tokyo) 51, 728 ~ 731, 2011

Reactivation of Hepatitis B Virus After Glioblastoma Treatment With Temozolomide

—Case Report—

Makoto OHNO,[1] Yoshitaka NARITA,[1] Yasuji MIYAKITA,[1] Hideki UENO,[2] Takamasa KAYAMA,[1] and Soichiro SHIBUI[1]

[1]Neurosurgery and Neuro-Oncology Division, and
[2]Hepatobiliary and Pancreatic Oncology Division, National Cancer Center Hospital, Tokyo

Abstract

A 61-year-old man with glioblastoma and positive for hepatitis B surface antigen (HBsAg) developed acute hepatitis due to hepatitis B virus (HBV) reactivation after concomitant postoperative treatment with temozolomide (75 mg/m^2/day) and radiation therapy (60 Gy in 30 fractions). Corticosteroids were not used during chemo-radiation therapy, and grade 4 lymphocytopenia was observed. The levels of liver function tests (LFTs), including levels of aspartate aminotransferase and alanine aminotransferase, increased 5 weeks after the completion of chemo-radiation therapy, and reached the maximum levels of 1,549 IU/l (normal 13 to 33 IU/l) and 1,653 IU/l (normal 8 to 42 IU/l), respectively, after 2 weeks. At this point, serum HBV-deoxyribonucleic acid (DNA) level had increased to 630-fold over the baseline, and therapy with the antivirus agent entecavir (0.5 mg daily) was started. Over the next 2 weeks, the levels of LFTs and HBV-DNA improved. The present and previous cases suggest that grade 3/4 lymphocytopenia or grade 2 lymphocytopenia with corticosteroid use might have a significant effect on HBV reactivation. To avoid this complication, HBsAg-positive patients with glioblastoma should consult a hepatologist for initiating antivirus therapy before temozolomide treatment.

Key words: hepatitis B virus, reactivation, glioblastoma, temozolomide, immunosuppression

Introduction

The reactivation of hepatitis B virus (HBV) is a well-recognized complication of cytotoxic chemotherapy for malignant disease. HBV reactivation usually occurs in patients with hematological malignancies, but is also known in patients with solid tumors, including breast cancer, gastrointestinal cancer, and lung cancer.[1,2]

Temozolomide is an alkylating agent that exerts cytotoxic activity by inducing deoxyribonucleic acid (DNA) damage and apoptosis of tumor cells,[7] and is part of the standard postoperative chemotherapy for the treatment of glioblastoma.[9] Temozolomide carries the risk of HBV reactivation,[1,2] but few cases of temozolomide-induced HBV reactivation have been reported, so the incidence and associated risk factors, and the optimal management of glioblastoma patients with chronic HBV infection remain unclear.

We treated a patient with glioblastoma who was positive for hepatitis B surface antigen (HBsAg) and developed acute hepatitis due to HBV reactivation during temozolomide treatment, and discuss the management of patients with glioblastoma who have chronic HBV infection.

Received December 24, 2010; Accepted March 24, 2011

Case Report

A 61-year-old man presented with generalized convulsions. He had been informed of his HBV carrier status but had not received any treatment. On admission, he tested positive for HBsAg and hepatitis B envelope (HBe) antibody, and negative for HBe antigen, hepatitis C virus antibody, and human immunodeficiency virus. The blood HBV-DNA concentration was 10^3 copies/ml. Magnetic resonance imaging of the brain showed a tumor in the bilateral frontal lobes involving the corpus callosum (Fig. 1A). The patient presented with slight disorientation and left hemiparesis. Partial tumor removal was achieved through a right frontal craniotomy, and the histological diagnosis was glioblastoma (Fig. 1B).

Betamethasone 8 mg was intravenously administered for 3 days following the operation. Ten days after resection, local radiation therapy (60 Gy in 30 fractions over 6 weeks) and temozolomide chemotherapy (75 mg/m^2/day) were initiated. Before chemotherapy and radiotherapy, the liver function tests (LFTs) were normal: aspartate aminotransferase (AST) was 26 IU/l (normal 13 to 33 IU/l), and alanine aminotransferase (ALT) was 28 IU/l (normal 8 to 42 IU/l). During chemo-radiation therapy, the lowest measured white blood cell count was 2900/μl, absolute neutrophil count was 2240/μl, and absolute lymphocyte

count was 190/μl. Four weeks after the completion of chemo-radiation therapy, the levels of LFTs started to increase, and one week later continued to deteriorate. AST increased to 685 IU/l and ALT increased to 744 IU/l. At this time we consulted with a hepatologist to determine the cause of the LFT changes. Abdominal computed tomography (CT) with contrast medium revealed a mass lesion in the liver (Fig. 2). Alpha fetoprotein (AFP) and protein induced by vitamin K or antagonists-II (PIVKA-II) were elevated to 257.6 ng/ml (normal <10.0 ng/ml) and 8,349 mAU/ml (normal <40 mAU/ml), respectively.

Our diagnosis was hepatocellular carcinoma (HCC) that had possibly developed before temozolomide treatment. Further, since the HCC was not obstructing the bile duct, we thought that the HCC was not the cause of the LFT changes. The patient's medication regimen at initial presentation consisted of valproic acid, propranolol, and famotidine. After the LFT changes, we stopped administration of famotidine but continued valproic acid and propranolol. The HBV-DNA level increased to $10^{5.8}$ copies/ml. On the basis of the laboratory data and radiological findings, we determined that temozolomide-induced HBV reactivation was the main cause of the LFT changes and acute hepatitis, although the possibility of drug-induced hepatitis or HCC-related LFT change was not completely excluded. Accordingly, we started treatment with the antivirus agent entecavir (0.5 mg daily). For 5 days after the start of entecavir treatment, AST and ALT continued to increase to the maximum levels of 1,549 IU/l and 1,653 IU/l, respectively, but thereafter improved markedly. Two weeks after the start of entecavir treatment, the LFTs returned to almost normal levels. The HBV-DNA level also decreased to $10^{1.8}$ copies/ml (Fig. 3).

After normalization of the LFTs, we started treatment with adjuvant temozolomide at 150 mg/m^2 daily for 5 days/28 days while continuing entecavir therapy. The second cycle used 200 mg/m^2 daily for 5 days/28 days, and no further elevation of LFTs and HBV-DNA level was observed, even though the lowest lymphocyte count was 110/μl (Fig. 3). Four weeks after the onset of LFT changes, the levels of AFP and PIVKA-II were 405.2 ng/ml and 10,195 mAU/ml, respectively, and continued to exacerbate his condition. Transarterial embolization was performed for the treatment of HCC. Three weeks later, the patient's AFP and PIVKA-II levels improved, decreasing to 166.4 ng/ml and 182 mAU/ml, respectively. However, after sec-

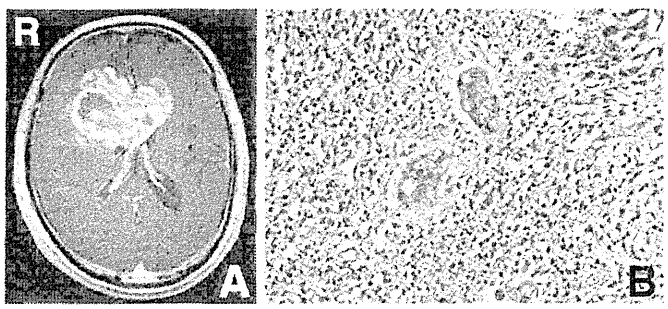

Fig. 1 A: Preoperative T_1-weighted magnetic resonance image with contrast medium showing a tumor in the bilateral frontal lobes involving the corpus callosum. B: Photomicrograph of the tumor specimen showing glioblastoma with cellular anaplasia and prominent microvascular proliferation. Hematoxylin and eosin stain, original magnification ×200.

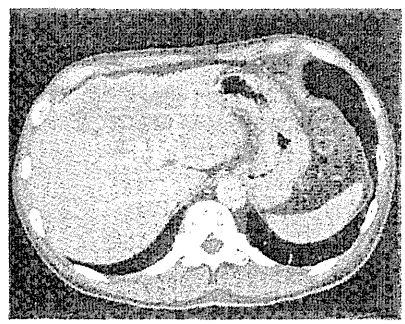

Fig. 2 Abdominal computed tomography scan with late phase contrast enhancement showing a low density mass lesion of 9-cm diameter in the liver.

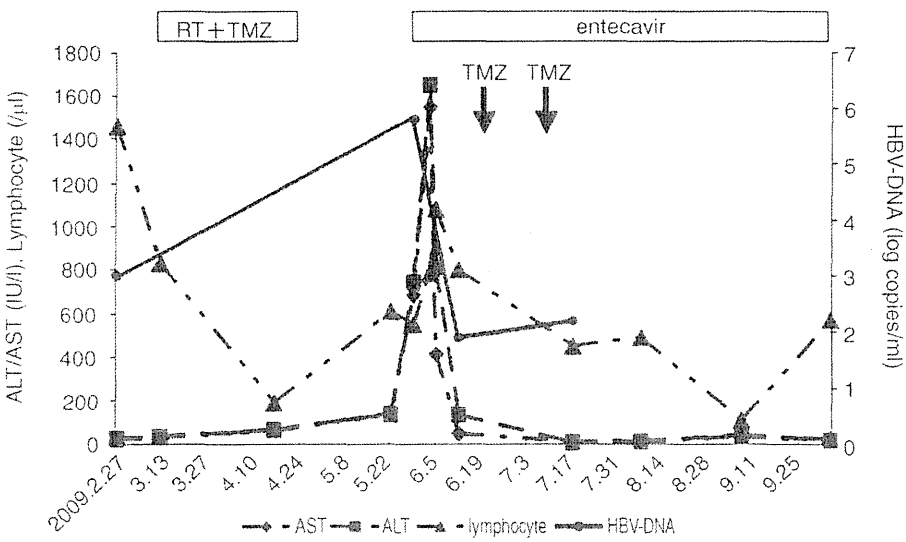

Fig. 3 Time courses of serum aspartate aminotransferase (AST), alanine aminotransferase (ALT), lymphocytes, and hepatitis B virus-deoxyribonucleic acid (HBV-DNA) levels. Four weeks after completion of concomitant temozolomide and radiation therapy (RT + TMZ), AST and ALT began to increase and continued to increase to a maximum of 1,549 IU/l and 1,653 IU/l, respectively. HBV-DNA level increased to $10^{5.8}$ copies/ml. After entecavir administration, ALT, AST, and HBV-DNA levels improved during the ensuing 2 weeks. After normalization of liver function, two cycles of adjuvant temozolomide (arrows) were initiated while continuing entecavir, without further elevation of AST and ALT even though the lowest lymphocyte count was 110/μl.

ond transarterial embolization, he developed conscious disturbance, and was transferred to a nursing hospital 6 months after the completion of chemo-radiation therapy. Twelve months after the neurosurgical operation, he died of glioblastoma progression.

Discussion

The reactivation of HBV by immunosuppressive agents is characterized by increased levels of serum HBV-DNA, abnormal LFTs, and clinical hepatitis of varying degrees of severity, which may result in death.[13] HBV reactivation occurs in 38–48% of HBsAg-positive patients with lymphoma or other hematological malignancies, who are undergoing conventional therapies, including cyclophosphamide, doxorubicin, vincristine, and prednisolone (CHOP).[4] The risk factors for HBV reactivation include male sex, young age, steroid use, anthracycline use, high pre-chemotherapy HBV-DNA level, and diagnosis of lymphoma or breast cancer.[3,12,13] Two possible mechanisms may explain HBV reactivation during chemotherapy: immunosuppression enhances virus replication, leading to hepatic toxicity, or chemotherapy-induced T-cell depletion dampens the host response to viral antigens, which enables broader hepatocyte infection, and following the subsequent withdrawal of cytotoxic chemotherapy, a rebound immune response results in hepatocyte destruction.[12]

HBV reactivation-induced hepatitis has been defined as an increase in HBV-DNA level to 10-fold or more when compared with the baseline level, or as an absolute increase in HBV-DNA level to more than $1,000 \times 10^6$ genome equivalents/ml in the absence of other systemic infections.[11] In our patient, the HBV-DNA level increased by 630-fold over the baseline, when the LFTs were elevated, indicating HBV reactivation. However, we could not completely exclude the possibility of drug-induced hepatitis or HCC-related LFT elevation, because the patient had received medication (valproic acid, propranolol, and famotidine) during chemotherapy just before the LFT changes and had underlying HCC. However, the patient continued to receive valproic acid and propranolol even after the LFTs were elevated. Abdominal CT did not reveal bile duct stenosis due to HCC, and both the LFTs and HBV-DNA level improved shortly after entecavir treatment before HCC therapy. Therefore, we presume that the possibility of drug-induced hepatitis or HCC-related increase in LFTs is much lower than that of HBV reactivation, although famotidine-induced hepatitis remains much less likely. Famotidine is also known to induce agranulocytosis[5] and can cause immunosuppression. However, the lowest white blood cell count and absolute neutrophil count in our patient were 2900/μl and 2240/μl, respectively, so the possibility of famotidine-induced agranulocytosis leading to HBV reactivation was thought to be quite low.

HBV infection is one of the causative factors in the development of HCC, and the patient probably had HCC before temozolomide treatment. However, HCC was unlikely to be involved in the development of HBV reactivation after temozolomide treatment, because HCC was localized at the time of increases in LFTs and did not impair the patient's general condition, including the immune system.

Only two cases of HBV reactivation after temozolomide treatment for glioblastoma have been reported (Table 1).[1,2] A 65-year-old woman with glioblastoma presented with HBV reactivation on day 27 of cycle 3 of adjuvant temozolomide therapy and died 2 weeks after the onset.[2] She had a remote history of hepatitis B infection but did not undergo hepatitis examination before starting treatment. She did not receive steroid medication before the onset of HBV reactivation, and her lowest lymphocyte count was 450/μl. A 50-year-old HBsAg-positive man with glioblastoma presented with HBV reactivation 5 weeks after the completion of concomitant radiotherapy and temozolomide.[1] He was successfully treated with the antiviral agent lamivudine over the ensuing 7 weeks. He was treated with 4 mg of dexamethasone during radiation therapy and 2 mg just before the onset of HBV reactivation. His lowest lymphocyte count was 580/μl. Our patient developed the symptoms 4 weeks after completing concomitant radiotherapy and temozolomide, and was successfully treated with entecavir during the ensuing 2 weeks. He had no steroid exposure before the onset of HBV reactivation, and his lowest lymphocyte count was 190/μl. All these cases suggest that grade 3/4 lymphocytopenia or grade 2 lymphocytopenia with corticosteroid use might have a significant effect on the development of HBV reactivation. The guidelines issued in the Joint Report of the Intractable Liver Disease Study Group of Japan and the Japanese Study Group of the Standard Antiviral Therapy for Viral Hepatitis recommend that all patients should be screened for HBsAg, and anti-hepatitis B core and anti-HBs antibodies before chemotherapy is initiated. HBsAg-positive patients should be advised to consult a hepatologist for initiating antiviral therapy, such as entecavir before starting chemotherapy.[10]

HBV reactivation after chemotherapy with temozolomide may be a rare complication. However, temozolomide is associated with $CD4^+$ T-cell dysfunction and therefore may cause increased susceptibility to opportunistic infections by agents such as *Pneumocystis* pneumonia.[8] This characteristic immunosuppression may also induce HBV reactivation. In the Japanese population, 1.4% of individuals are positive for HBsAg,[6] so HBV reactivation during glioblastoma treatment with temozolomide may become a critical issue. To avoid this complication, patients with glioblastoma should be screened for hepatitis B, and HBsAg-positive patients should be referred to a hepatologist for initiating antivirus therapy before starting temozolomide treatment. Moreover, HBV reactivation should be included in the differential diagnosis of patients with elevated LFTs.

References

1) Chheda MG, Drappatz J, Greenberger NJ, Kesari S, Weiss SE, Gigas DC, Doherty LM, Wen PY: Hepatitis B reactivation during glioblastoma treatment with temozolomide: a

Table 1 Summary of three cases of hepatitis B virus (HBV) reactivation induced by temozolomide (TMZ)

Author (Year)	Age (yrs)/ Sex	HBV status	Diagnosis	Onset	Nadir			Steroid	Status of hepatitis
					WBC (/μl)	Neutrophil (/μl)	Lymphocyte (/μl)		
Grewal et al. (2007)[2]	65/F	remote history of HBV infection, not determined by laboratory test	GBM	day 27 of cycle 3	N/A	1250	450	stop 1 week after operation	died of hepatitis 2 weeks after onset
Chheda et al. (2007)[11]	50/M	HBsAg (+)	GBM	5 weeks after completion of TMZ concomitant with RT	5300	3890	580	dexamethasone 4 mg 5 weeks before onset and 2 mg at onset	successfully treated with lamivudine over the next 7 weeks
Present case	61/M	HBsAg (+)	GBM	4 weeks after completion of TMZ concomitant with RT	2900	2240	190	stop 3 days after operation	successfully treated with entecavir over the next 2 weeks

F: female, GBM: glioblastoma, HBsAg: hepatitis B surface antigen, M: male, N/A: not available, RT: radiation therapy, WBC: white blood cell.

cautionary note. *Neurology* 68: 955–956, 2007
2) Grewal J, Dellinger CA, Yung WK: Fatal reactivation of hepatitis B with temozolomide. *N Engl J Med* 356: 1591–1592, 2007
3) Lok AS, Liang RH, Chiu EK, Wong KL, Chan TK, Todd D: Reactivation of hepatitis B virus replication in patients receiving cytotoxic therapy. Report of a prospective study. *Gastroenterology* 100: 182–188, 1991
4) Lubel JS, Testro AG, Angus PW: Hepatitis B virus reactivation following immunosuppressive therapy: guidelines for prevention and management. *Intern Med J* 37: 705–712, 2007
5) Marcus EL, Clarfield AM, Kleinman Y, Bits H, Darmon D, Da'as N: Agranulocytosis associated with initiation of famotidine therapy. *Ann Pharmacother* 36: 267–271, 2002
6) Nakamura Y, Motokura T, Fujita A, Yamashita T, Ogata E: Severe hepatitis related to chemotherapy in hepatitis B virus carriers with hematologic malignancies. Survey in Japan, 1987–1991. *Cancer* 78: 2210–2215, 1996
7) Newlands ES, Stevens MF, Wedge SR, Wheelhouse RT, Brock C: Temozolomide: a review of its discovery, chemical properties, pre-clinical development and clinical trials. *Cancer Treat Rev* 23: 35–61, 1997
8) Schwarzberg AB, Stover EH, Sengupta T, Michelini A, Vincitore M, Baden LR, Kulke MH: Selective lymphopenia and opportunistic infections in neuroendocrine tumor patients receiving temozolomide. *Cancer Invest* 25: 249–255, 2007
9) Stupp R, Mason WP, van den Bent MJ, Weller M, Fisher B, Taphoorn MJ, Belanger K, Brandes AA, Marosi C, Bogdahn U, Curschmann J, Janzer RC, Ludwin SK, Gorlia T, Allgeier A, Lacombe D, Cairncross JG, Eisenhauer E, Mirimanoff RO: Radiotherapy plus concomitant and adjuvant temozolomide for glioblastoma. *N Engl J Med* 352: 987–996, 2005
10) Tsubouchi H, Kumada H, Kiyosawa K, Mochida S, Sakaida I, Tanaka E, Ichida T, Mizokami M, Suzuki K, Yoshiba S, Moriwaki H, Hibi T, Hayashi N, Kokudo N, Fujisawa T, Ishibashi H, Sugawara Y, Yatsuhashi H, Ido A, Takikawa Y, Inoue K, Oketani M, Uto H, Nakayama N, Naiki T, Tada S, Kiso S, Yano K, Endo R, Tanaka Y, Umemura T, Kumagai K: [Prevention of immunosuppressive therapy or chemotherapy-induced reactivation of hepatitis B virus infection—Joint report of the Intractable Liver Diseases Study Group of Japan and the Japanese Study Group of the Standard Antiviral Therapy for Viral Hepatitis]. *Kanzo* 50: 38–42, 2009 (Japanese)
11) Yeo W, Chan PK, Ho WM, Zee B, Lam KC, Lei KI, Chan AT, Mok TS, Lee JJ, Leung TW, Zhong S, Johnson PJ: Lamivudine for the prevention of hepatitis B virus reactivation in hepatitis B s-antigen seropositive cancer patients undergoing cytotoxic chemotherapy. *J Clin Oncol* 22: 927–934, 2004
12) Yeo W, Chan PK, Zhong S, Ho WM, Steinberg JL, Tam JS, Hui P, Leung NW, Zee B, Johnson PJ: Frequency of hepatitis B virus reactivation in cancer patients undergoing cytotoxic chemotherapy: a prospective study of 626 patients with identification of risk factors. *J Med Virol* 62: 299–307, 2000
13) Yeo W, Zee B, Zhong S, Chan PK, Wong WL, Ho WM, Lam KC, Johnson PJ: Comprehensive analysis of risk factors associating with Hepatitis B virus (HBV) reactivation in cancer patients undergoing cytotoxic chemotherapy. *Br J Cancer* 90: 1306–1311, 2004

Address reprint requests to: Makoto Ohno, MD, PhD, Neurosurgery and Neuro-Oncology Division, National Cancer Center Hospital, 5-1-1 Tsukiji, Chuo-ku, Tokyo 104-0045, Japan.
e-mail: mohno@ncc.go.jp

Stem Cell Research (2014) 12, 119–131

Available online at www.sciencedirect.com

ScienceDirect

www.elsevier.com/locate/scr

Pivotal role for ROS activation of p38 MAPK in the control of differentiation and tumor-initiating capacity of glioma-initiating cells☆

Atsushi Sato[a,b,*], Masashi Okada[a], Keita Shibuya[a,c,d], Eriko Watanabe[a,c,d], Shizuka Seino[a,c,d], Yoshitaka Narita[e], Soichiro Shibui[e], Takamasa Kayama[b], Chifumi Kitanaka[a,c,d,*]

[a] *Department of Molecular Cancer Science, Yamagata University School of Medicine, Yamagata 990-9585, Japan*
[b] *Department of Neurosurgery, Yamagata University School of Medicine, Yamagata 990-9585, Japan*
[c] *Oncology Research Center, Research Institute for Advanced Molecular Epidemiology, Yamagata University, Yamagata 990-9585, Japan*
[d] *Global COE Program for Medical Sciences, Japan Society for the Promotion of Science, Tokyo 102-8471, Japan*
[e] *Department of Neurosurgery and Neuro-Oncology, National Cancer Center Hospital, Tokyo 104-0045, Japan*

Received 11 March 2013; received in revised form 5 August 2013; accepted 23 September 2013
Available online 4 October 2013

Abstract Reactive oxygen species (ROS) are involved in various aspects of cancer cell biology, yet their role in cancer stem cells (CSCs) has been poorly understood. In particular, it still remains unclear whether and how ROS control the self-renewal/differentiation process and the tumor-initiating capacity of CSCs. Here we show that ROS-mediated activation of p38 MAPK plays a pivotal role in the control of differentiation and tumor-initiating capacity of glioma-initiating cells (GICs) derived from human glioblastomas. Mechanistically, ROS triggered p38-dependent Bmi1 protein degradation and FoxO3 activation in GICs, which were shown to be responsible for the loss of their self-renewal capacity and differentiation, respectively. Thus, the results suggest that Bmi1 and FoxO3 govern distinct phases of transition from undifferentiated to fully differentiated cells. Furthermore, we also demonstrate in this study that oxidative stress deprives GICs of their tumor-initiating capacity through the activation of the ROS–p38 axis. As such, this is the first study to the best of our knowledge to delineate how ROS control self-renewal/differentiation and the tumor-initiating capacity of stem-like cancer cells. This study also suggests that targeting of the ROS–p38 axis could be a novel approach in the development of therapeutic strategies against gliomas, represented by glioblastoma.

Abbreviations: BSO, L-buthionine-sulfoximine; CSC, cancer stem cell; DCF-DA, 2′,7′-dichlorofluorescein diacetate; GFAP, glial fibrillary acidic protein; GIC, glioma-initiating cell; GSH, glutathione; NAC, N-acetylcysteine; ROS, reactive oxygen species

* Corresponding authors at: Department of Molecular Cancer Science, Yamagata University School of Medicine, Yamagata 990-9585, Japan. Fax: +81 23 628 5215.
E-mail addresses: asato@med.id.yamagata-u.ac.jp (A. Sato), ckitanak@med.id.yamagata-u.ac.jp (C. Kitanaka).

1873-5061/$ - see front matter © 2013 The Authors. Published by Elsevier B.V. All rights reserved.
http://dx.doi.org/10.1016/j.scr.2013.09.012

Introduction

Glioblastoma is one of the deadliest among human cancers with highly dismal prognosis (Stupp et al., 2005; Tabatabai and Weller, 2011). Even with seemingly successful initial treatment, recurrence is inevitable and almost always fatal in the majority of glioblastoma cases, which implies that the control of recurrence is key to realizing long-term survival of glioblastoma patients (Cheng et al., 2010; Neman and Jandial, 2010). A growing body of evidence now suggests that glioblastomas contain a small subpopulation of immature, undifferentiated tumor cells with tumor-initiating capacity, which is lost once they undergo differentiation (Binello and Germano, 2011; Cheng et al., 2010; Tabatabai and Weller, 2011). Such cells are called glioma stem cells (or alternatively, stem-like glioma cells, glioma-initiating cells [GICs], glioma-propagating cells), and due to their inherent therapy resistance, are now deemed a possible culprit of glioblastoma recurrence (Binda et al., 2012). Elucidation of the molecular mechanisms underlying the maintenance of the immature, stem cell state of glioma stem cells as well as the process of their differentiation, therefore, is expected to lead to the identification of novel targets of therapeutic intervention to prevent recurrence and thus could contribute to better clinical management of this devastating disease.

Currently, with the dramatic expansion of research in the field of glioma stem cells, an increasing number of molecules/pathways involved in their maintenance and differentiation, e.g., bone morphogenetic proteins and transforming growth factor β, are being identified (Binello and Germano, 2011). However, the role of reactive oxygen species (ROS) in cancer stem cells, including glioma stem cells, has been poorly characterized with only limited information published to date (Kobayashi and Suda, 2012), in contrast to their well-documented, pleiotropic roles in cancer cell biology in general (Pan et al., 2009). In particular, although previous studies implicated ROS in the radioresistance of breast cancer stem cells (Diehn et al., 2009; Phillips et al., 2006), the role of ROS in the control of stem cell state/differentiation of cancer stem cells remains largely undetermined (Shi et al., 2012).

Here in this study, to address this important, unanswered question, we investigated the role of ROS in GICs having stem-like properties (stem-like GICs). We found that p38 MAPK activated by ROS mediates the loss of self-renewal and differentiation of stem-like GICs induced by oxidative stress. Intriguingly, we also found that Bmi1 and FoxO3 under the control of this ROS–p38 axis play critical roles at distinct phases of transition from the undifferentiated to differentiated state. The pivotal role of the ROS–p38 axis in the control of stem-like GICs and their tumor-initiating capacity demonstrated in this study suggests that the axis may be a novel node for therapeutic targeting of stem-like GICs.

Materials and methods

Reagents and antibodies

Hydrogen peroxide solution (H_2O_2, #216763), *N*-acetyl-L-cysteine (NAC, #A9165), L-buthionine-sulfoximine (BSO, #B2515), 2′,7′-dichlorofluorescein diacetate (DCF-DA, #35845), cycloheximide solution (#C4859) and SB203580 (#S8307) were purchased from Sigma-Aldrich. MG132 (#BML-PI102) and SL327 (#EI-365) were from Enzo Life Sciences. LY294002 (#440202) was purchased from Calbiochem. Hoechst33342 (#H3570) was from Invitrogen.

The following antibodies were used: Anti-Nestin (#AB5922), Anti-Neurofilament H (#MAB5446) and Anti-Bmi-1 (#05-637) from Millipore; SOX2 (#MAB2018), GFAP (#AF2594), and βIII-tubulin (#MAB1195) from R&D Systems; and phospho-Akt (#4058), Akt (#9272), phospho-ATF-2 (#9221), ATF-2 (#9222), phospho-Erk1/2 (#9106), Erk1/2 (#4695), FoxO3a (#2497), phospho-p38 (#4511), p38 (#9212), p21 (#2947) and PARP (#9542) from Cell Signaling Technology. Anti-α-tubulin (#CP06) was from Oncogene. Anti-Musashi-1 (#ab21628) was from Abcam. Anti-β-actin (#A1978) was from Sigma-Aldrich. HRP-conjugated secondary antibodies for immunoblotting were purchased from Jackson ImmunoResearch Laboratories. Alexa 488- and 568-conjugated secondary antibodies for immunocytochemistry were from Invitrogen.

Culture of GICs and sphere formation assay

Patient-derived GICs used in this study were directly established from glioblastoma tissues in accordance with a protocol approved by the Institutional Review Boards of Yamagata University School of Medicine and National Cancer Center (GS-Y03, GS-NCC01) (Matsuda et al., 2012; Sunayama et al., 2010a, 2010b, 2011) or were kindly provided by Drs. Tomoki Todo and Nobuhito Saito at the University of Tokyo (TGS01) (Ikushima et al., 2009; Matsuda et al., 2012; Sato et al., 2011). The patient-derived GICs were maintained under the monolayer stem cell culture condition reported previously, and the determination of the cell number and viability was also carried out essentially as described (Matsuda et al., 2012; Sato et al., 2012).

Unless otherwise indicated, sphere formation assay was done essentially as previously described (Matsuda et al., 2012; Sato et al., 2012). Monolayer-cultured GICs were, after being detached from the dish and dissociated into single cells mechanically (i.e., by pipetting), suspended in the stem cell culture medium at a density of 5×10^3 cells/ml. Then, 200 μl of the cell suspension (1×10^3 cells) was transferred to each well of a non-coated 96-well plate. The number of primary spheres was counted after 3 (TGS01) or 6 (GS-Y03 and GS-NCC01) days. For secondary sphere formation, primary spheres formed by cells seeded onto non-coated 35-mm dishes at a density of 5×10^3 cells/ml in the stem cell culture medium were collected 3 days after seeding, dissociated, and 200 μl of the cell suspension (5×10^3 cells/ml in the stem cell culture medium) was transferred to each well of a non-coated 96-well plate. Secondary spheres were similarly counted after 3 (TGS01) or 6 (GS-Y03 and GS-NCC01) days. Tertiary sphere formation assay was performed essentially in the same manner as the primary and secondary sphere formation assays. Where indicated, the sphere formation capacity of GICs was also assessed by limiting dilution. Cells were diluted in the stem cell culture medium and seeded so that there will be a single cell in each well of non-coated 96-well plates. After seeding, wells containing a single cell were marked, and

the percentage of marked wells with a sphere relative to the total number of marked wells was determined 7 days after seeding.

Detection and measurement of intracellular ROS

Cells were incubated with the stem cell culture medium containing 10 μM 2′,7′-dichlorofluorescein diacetate (DCF-DA) for 10 min at 37 °C, washed twice with phosphate-buffered saline, and fixed with 4% (w/v) paraformaldehyde for 5 min at room temperature. Care was taken to shield light during these procedures. The cells were then subjected either to fluorescence microscopy using an epifluorescence microscope (CKX41; Olympus) equipped with a CCD camera system (DP-30BW; Olympus) or to flow cytometric analysis for quantification of the intensity of DCF fluorescence using a BD FACSCalibur flow cytometer (Becton Dickinson). For flow cytometric analysis, at least 5×10^5 cells were evaluated and gated using side and forward scatters to identify live cell populations.

Gene silencing by siRNA

Monolayer-cultured GICs seeded at a density of 2×10^5 cells/ml in the stem cell culture medium on collagen-coated dishes were transfected with siRNAs using Lipofectamine RNAiMAX Reagent (Invitrogen). siRNAs against MAPK14 (p38α) (p38-#1 [HSS102352] and p38-#2 [HSS102353]), siRNAs against Bmi1 (Bmi1-#1 [HSS101038] and Bmi1-#2 [HSS101039]), and a non-targeting control siRNA (Stealth RNAi™ siRNA Negative Control Duplexes [Medium GC Duplexes #2, 12935112]) were purchased from Invitrogen.

Immunoblot analysis

Cells were washed with phosphate-buffered saline and then lysed in the lysis buffer (10 mM Tris–HCl, pH 7.4, 0.1% (w/v) SDS, 1% (w/v) sodium deoxycholate, 0.15 M NaCl, 1 mM EDTA, and 1% (v/v) protease inhibitor cocktail set III; Merck). After determination of the protein concentrations by using a BCA protein assay kit (Thermo Fisher Scientific), cell lysates containing equal amounts of protein were separated by SDS-PAGE and electrically transferred to polyvinylidene difluoride membranes. The membrane was probed with a primary antibody and then with an appropriate HRP-conjugated secondary antibody. Blots were visualized with Immobilon Western HRP Substrate (Millipore) or ECL Western Blotting Detection Reagent (GE Healthcare).

Subcellular fractionation

Cells were homogenized in hypotonic buffer (10 mM Tris–HCl, pH 7.8, 150 mM NaCl, and 1 mM EDTA) containing 0.1% (w/v) Triton X-100. The lysates were centrifuged at 3000 rpm for 10 min at 4 °C and separated into pellet and supernatant fractions. The pellet was re-suspended in hypotonic buffer containing 0.1% (v/v) Triton X-100 and re-centrifuged. The pellet was used as the nuclear fraction. The supernatant fraction was re-centrifuged at 15,000 rpm for 20 min at 4 °C and used as the cytoplasmic fraction.

Immunofluorescence

Cells were plated onto collagen-coated coverslips (Iwaki) in the stem cell culture medium and fixed with 4% (w/v) paraformaldehyde for 30 min at room temperature. The fixed cells were permeabilized in 0.5% (w/v) Triton X-100 for 5 min, washed twice with PBS, and incubated in a blocking solution (phosphate-buffered saline containing 2% (w/v) bovine serum albumin and 2% (v/v) fetal bovine serum) for 30 min. The cells were incubated in the blocking solution with the primary antibodies overnight at 4 °C and then with the secondary antibodies for 1 h at room temperature. Immune complexes were observed under an epifluorescence microscope (CKX41; Olympus) equipped with a CCD camera system (DP-30BW; Olympus).

RT-PCR analysis

Total RNA was extracted with TRIzol (Invitrogen). Total RNA was reverse-transcribed into cDNA using M-MLV (Invitrogen) according to the manufacturer's instruction.

RT-PCR analysis was performed with the following primers.

bmi1 (F; 5′-GGAGACCAGCCAGTATTGTCCTATTTG-3′, R; 5′-CATTGCTGCTGGGCATCGTAAG-3′)
gapdh (F; 5′-TCCTGTTCGACAGTCAGCCGCATCTT-3′, R; 5′-GACCAGGCGCCCAATACGACCAA-3′)

Mouse xenograft analysis

For intracranial xenografts, monolayer-cultured GS-Y03 cells (1×10^4) in 10 μl PBS were injected stereotactically into the right corpus striatum (2.5 mm anterior and 2.5 mm lateral to the bregma, and 3.0 mm deep) of 5-week-old male BALB/cAJcl-*nu*/*nu* mice (CLEA Japan). All animal experiments were performed under the approval of the Animal Research Committee of Yamagata University.

Statistical analysis

Quantitative data are expressed as means ± SD, and differences were compared using two-tailed Student's *t*-test. Mouse survival was evaluated by the Kaplan–Meier method and analyzed by using the log-rank test. *P* values less than 0.05 were considered statistically significant.

Results

Hydrogen peroxide inhibits self-renewal and induces differentiation of GICs via increase in intracellular ROS

The results of pilot experiments in our recent study indicated that hydrogen peroxide treatment induces differentiation of a patient-derived GIC, GS-NCC01 (previously designated SJ28P3), in a FoxO3-dependent manner (Sunayama et al., 2011), which suggested the possibility that intracellular ROS elevation as a result of oxidative stress caused by hydrogen peroxide may play a role in the differentiation of the GIC. To test this idea and whether the mechanism is shared by other GICs, we

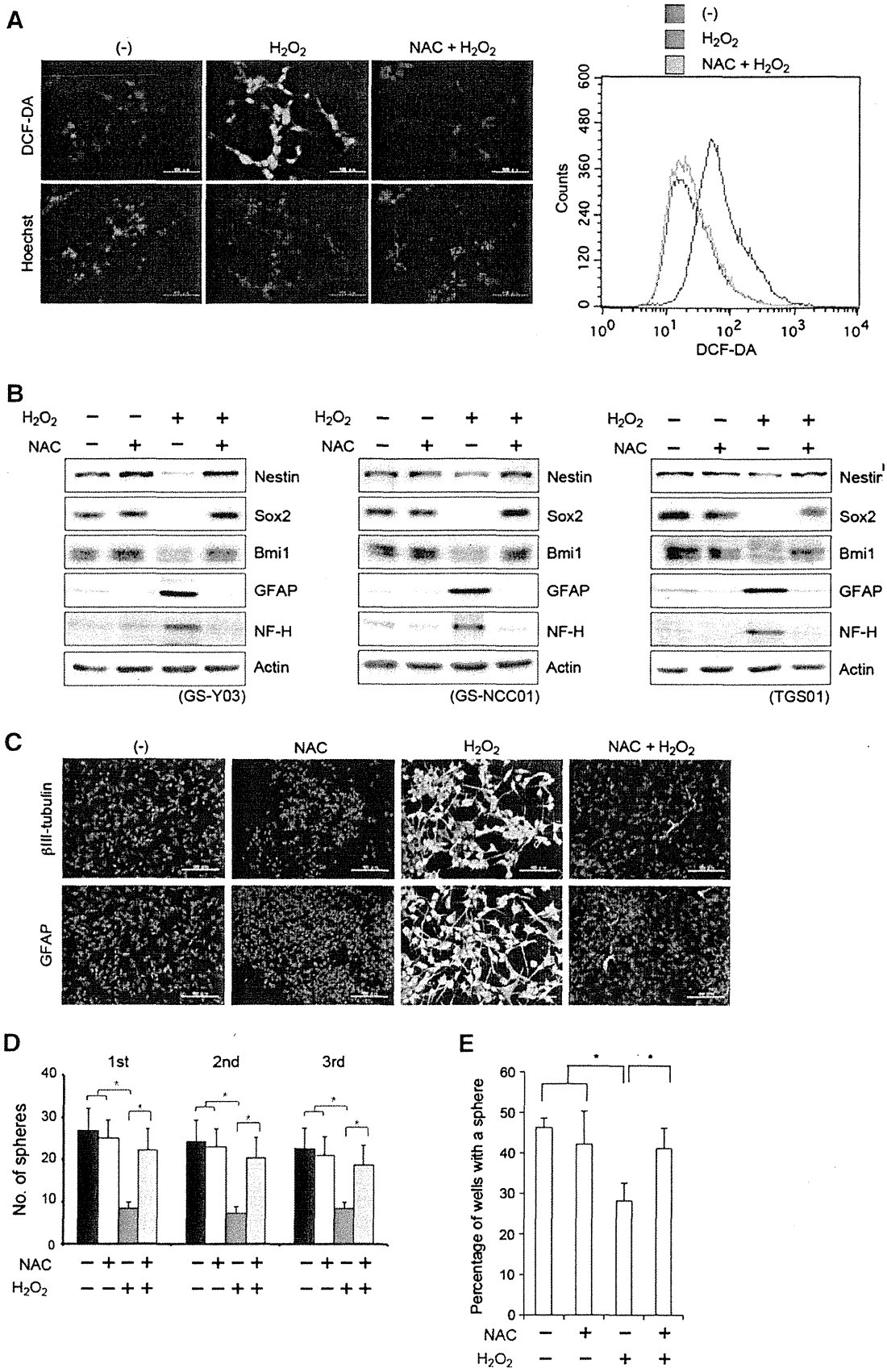
A
(-)
H2O2
NAC + H2O2
DCF-DA
Hoechst
Counts
DCF-DA
B
Nestin
Sox2
Bmi1
GFAP
NF-H
Actin
(GS-Y03)
(GS-NCC01)
(TGS01)
C
βIII-tubulin
GFAP
NAC
D
1st
2nd
3rd
No. of spheres
E
Percentage of wells with a sphere

examined the effect of hydrogen peroxide treatment on three patient-derived GICs (including GS-NCC01) established in three different institutions (Fig. 1). When the GICs were treated with hydrogen peroxide at different concentrations and the intracellular ROS levels were measured by DCF-DA staining, we found that the extent of increase in the intracellular ROS levels varied depending on the GIC examined. Nevertheless, when the cells were treated with hydrogen peroxide at 100 μM or higher concentrations, we could consistently detect significant elevation of the intracellular ROS levels in all three GICs (Fig. 1; Figs. S2 and S12). In the following experiments, therefore, the experiments were conducted using 100 μM hydrogen peroxide unless otherwise indicated. To determine whether hydrogen peroxide induces differentiation of the GICs, and if so, through elevation of the intracellular ROS levels, we treated the GICs (GS-NCC01, GS-Y03, and TGS01) with 100 μM hydrogen peroxide in the presence and absence of an antioxidant N-acetylcysteine (NAC), which acts as a free radical scavenger by promoting intracellular biosynthesis of glutathione (GSH) (Kelly, 1998). Treatment of GICs with 100 μM hydrogen peroxide resulted in increased intracellular ROS as early as 30 min after treatment, and the intracellular ROS level remained above the baseline for 48 h (Fig. S1). Under this treatment condition, hydrogen peroxide reduced sphere formation by GICs (Figs. 1D and E; Fig. S2C) without causing substantial reduction in their viability (Fig. S3), and also reduced their stem cell marker expression (Nestin, Sox2, Bmi1) while inducing expression of differentiation markers such as GFAP, neurofilament H (NF-H) (Fig. 1B) and βIII-tubulin (Fig. 1C; Fig. S2B), in all three GICs. Importantly, NAC, which completely inhibited hydrogen peroxide-induced elevation of the intracellular ROS levels (Fig. 1A; Fig. S2A), almost totally canceled the effect of hydrogen peroxide on the sphere forming capacity (Fig. 1D; Fig. S2C) and stem cell/differentiation marker expression (Figs. 1B and C; Fig. S2B) of the GICs. These results indicate that hydrogen peroxide inhibits self-renewal and induces differentiation of stem-like GICs by increasing intracellular ROS.

Hydrogen peroxide inhibits self-renewal and induces differentiation of GICs via ROS-dependent activation of p38 MAPK

Next, to identify the signaling pathway(s) involved in ROS-mediated differentiation of GICs, we first searched for candidate signaling pathways that could be activated or inhibited in a ROS-dependent manner. As we reported previously (Sunayama et al., 2011), the activity of the MAPK pathway as assessed by phosphorylated ERK remained unchanged when cells were treated with hydrogen peroxide in the presence and absence of NAC. Of note, in contrast to our previous report (Sunayama et al., 2011), a modest increase in phosphorylated Akt was observed upon hydrogen peroxide treatment, most likely due to the higher concentration (100 μM vs. 10 μM) of hydrogen peroxide used in this study to achieve a significant increase in the intracellular ROS levels in all three GICs (Fig. 2A; Fig. S4A). Quite intriguingly, we noticed in the course of our experiments that phosphorylation of p38 MAPK was commonly increased in all the GICs examined, apparently in a ROS-dependent manner as evidenced by its inhibition by NAC (Fig. 2A; Fig. S4A). Then, to determine whether p38 is indeed involved in hydrogen peroxide-induced differentiation and loss of self-renewal, we investigated the effect of p38 knockdown on the stem-like properties of the GICs, using two different siRNAs against p38. Both siRNAs effectively knocked down p38 and prevented hydrogen peroxide-induced activation of p38 (Fig. 2C; Fig. S5A). Under this experimental condition, the siRNAs against p38 blocked hydrogen peroxide-induced differentiation (Fig. 2C; Fig. S5A) and loss of self-renewal (Figs. 2C and E; Figs. S5A and B). The results of the knockdown study were further corroborated by the use of SB203580, a pharmacological inhibitor of p38. SB203580 prevented hydrogen peroxide-induced expression of differentiation markers (Fig. 2D; Fig. S6B), suggesting that p38 is required for hydrogen peroxide-induced differentiation of GICs. Similarly, SB203580 effectively blocked hydrogen peroxide-induced reduction in stem cell marker expression (Fig. 2D; Fig. S6B) and sphere formation (Fig. S4B) of GICs, demonstrating that p38 is responsible for the loss of self-renewal induced by hydrogen peroxide. Of note, SB203580 did not affect the intracellular ROS levels (Fig. 2B; Fig. S6A), consistent with the idea that p38 functions downstream of ROS in GICs. Collectively, these data indicate that ROS-dependent activation of p38 is essential for both loss of self-renewal and differentiation of GICs induced by hydrogen peroxide.

Downregulation of Bmi1 expression precedes alteration of stem cell/differentiation marker expression induced by hydrogen peroxide and is sufficient to cause loss of self-renewal but not differentiation of GICs

In an attempt to obtain clues to further delineate the mechanism underlying hydrogen peroxide-induced differentiation of GICs, we conducted a time course analysis of

Figure 1 Hydrogen peroxide treatment inhibits self-renewal and induces differentiation of GICs via increase in intracellular ROS. (A) GS-Y03 cells cultured in the presence or absence of NAC (10 mM) for 30 min were further treated with or without H_2O_2 (100 μM) for another 30 min. The cells were then stained with DCF-DA and subjected to fluorescence microscopy after nuclear staining with Hoechst 33342 (Hoechst) (left panels; identical visual fields are shown for each pair of DCF-DA and Hoechst staining) or to flow cytometry (right panel), to detect intracellular ROS. Scale bars, 100 μm. (B) The indicated GICs cultured in the presence or absence of NAC (10 mM) for 30 min were further treated with or without H_2O_2 (100 μM) for 6 days. The cells were then subjected to immunoblot analysis for the expression of stem cell and differentiation markers. (C) GS-Y03 cells were treated as in (B) and subjected to immunofluorescence analysis for GFAP and βIII-tubulin expression (green). Nuclei were counter-stained with Hoechst 33342 (blue). Scale bars, 100 μm. (D) GS-Y03 cells treated as in (B) were subjected to sphere formation assay to determine the number of spheres formed. The data represent means ± SD from 3 independent experiments. (E) GS-Y03 cells treated as in (B) were assessed for their sphere forming capacity by limiting dilution. The graph shows the percentage of wells with a sphere, and the data represent means ± SD from 3 independent experiments.

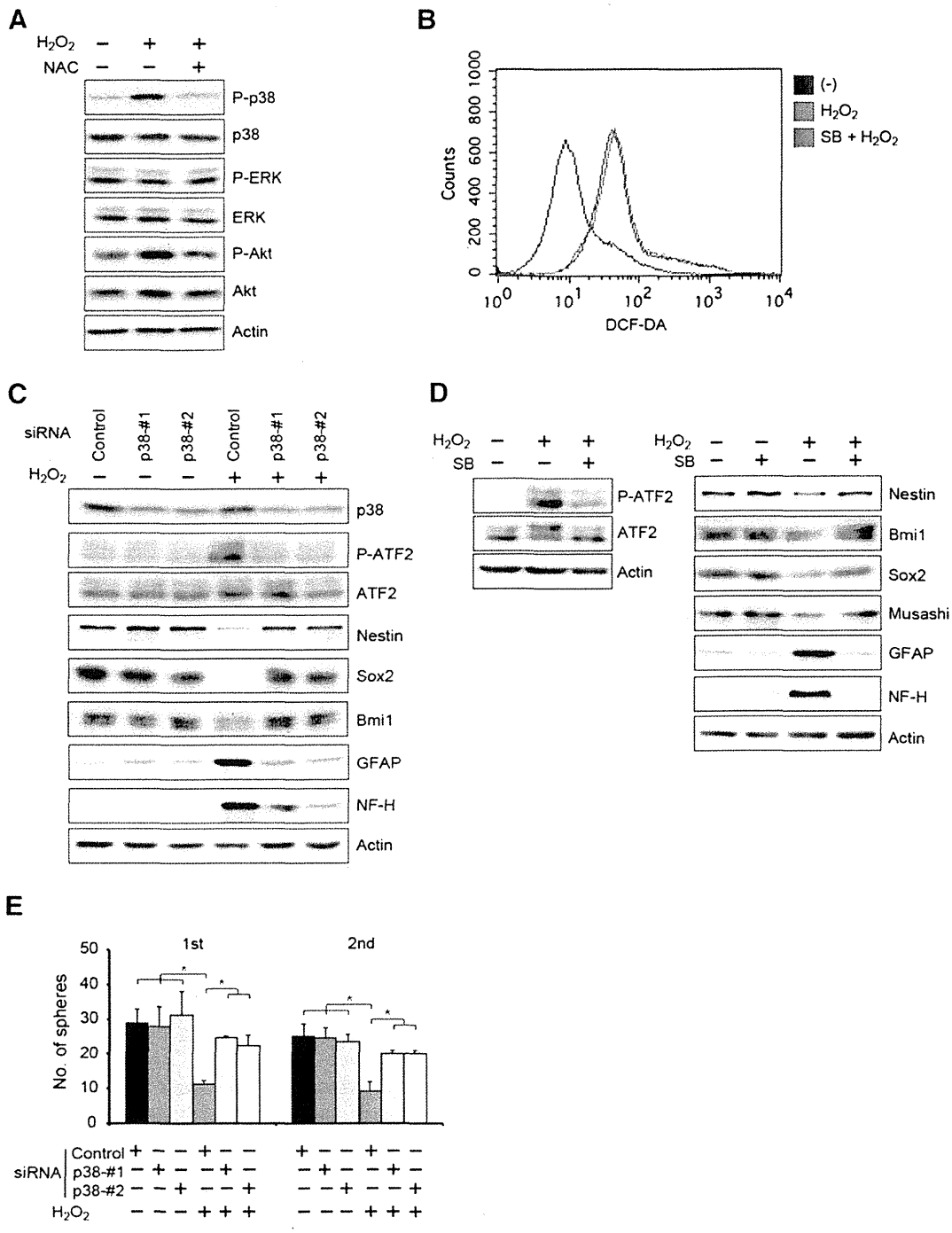

Figure 2 Hydrogen peroxide inhibits self-renewal and induces differentiation of GICs via intracellular ROS-dependent activation of p38 MAPK. (A) GS-Y03 cells cultured in the presence or absence of NAC (10 mM) for 30 min were further treated with or without H_2O_2 (100 μM) for 1 h. The cells were then subjected to immunoblot analysis of the indicated proteins. (B) GS-Y03 cells cultured in the presence or absence of SB203580 (SB) for 30 min were further treated with or without H_2O_2 (100 μM) for another 30 min. Then the cells were stained with DCF-DA and analyzed by flow cytometry. (C) GS-Y03 cells were transfected with the indicated siRNAs. After 10 h, the transfected cells were treated with or without H_2O_2 (100 μM) for 6 days and then subjected to immunoblot analysis. (D) GS-Y03 cells cultured in the presence or absence of SB203580 (SB) were further treated with or without H_2O_2 (100 μM) for 6 days. The cells were then subjected to immunoblot analysis. (E) GS-Y03 cells were treated as in (C) and then subjected to sphere formation assays. The data represent means ± SD from 3 independent experiments.

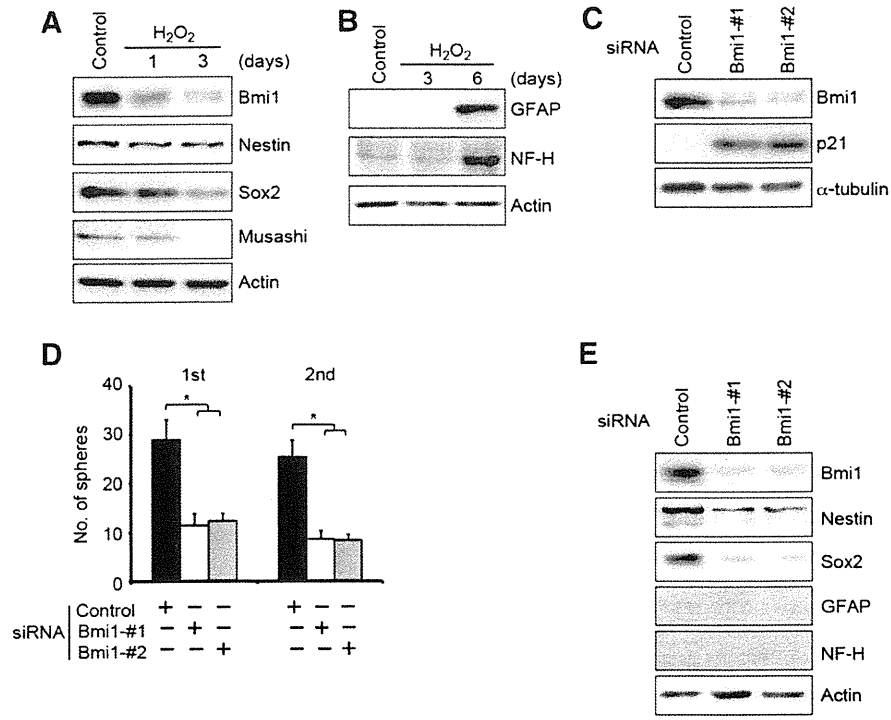

Figure 3 Downregulation of Bmi1 expression precedes alteration of stem cell/differentiation marker expression induced by hydrogen peroxide and is sufficient to cause loss of self-renewal but not differentiation of GICs. (A, B) GS-Y03 cells cultured in the absence (Control) or presence of H_2O_2 (100 μM) for the indicated time periods were subjected to immunoblot analysis for the expression of stem cell (A) and differentiation (B) markers. (C–E) GS-Y03 cells transfected with the indicated siRNAs were, 6 days after transfection, subjected to immunoblot analyses (C and E) or to sphere formation assays (D). In (D), the data represent means ± SD from 3 independent experiments.

stem cell/differentiation marker expression. Under the experimental condition of this study, decreased expression of Bmi1, a stem cell marker, was already apparent at 1 day after hydrogen peroxide treatment, whereas the expression of the other stem cell markers (Sox2, Musashi, Nestin) began to decline between 1 and 3 days after hydrogen peroxide treatment (Fig. 3A; Fig. S7A). The expression of differentiation markers became detectable later than 3 days and was invariably robust at 6 days after hydrogen peroxide treatment (Fig. 3B; Fig. S7B). Thus, the results of the time course analysis suggested that the process of hydrogen peroxide-induced differentiation of the GICs is preceded by the downregulation of Bmi1 followed by other stem cell markers, and then by the upregulation of differentiation markers. Given a previous report showing that Bmi1 expression is required for the maintenance of the undifferentiated state of GICs (Abdouh et al., 2009), we hypothesized that the initial downregulation of Bmi1 may serve as a cue for the subsequent downregulation of the other stem cell markers and upregulation of the differentiation markers. To test this possibility, we investigated the impact of Bmi1 knockdown on stem cell/differentiation marker expression as well as on the sphere formation capacity of the GICs. When Bmi1 was knocked down using two different siRNAs, upregulation of p21, a Bmi1 target, was confirmed along with reduced expression of Bmi1, implying that both siRNAs knocked down Bmi1 effectively in the GICs (Fig. 3C; Fig. S7C). Then, under this experimental condition, the GICs with or without Bmi1 knockdown were subjected to sphere formation assay or to analysis of stem cell/differentiation marker expression. As expected, Bmi1 knockdown caused substantial reduction in sphere formation (Fig. 3D; Fig. S7D) and stem cell marker expression (Fig. 3E; Fig. S7E). However, unexpectedly, we failed to detect the expression of differentiation markers even at 6 days after Bmi1 knockdown (Fig. 3E; Fig. S7E). Thus, the data suggested that the downregulation of Bmi1 caused by hydrogen peroxide may be sufficient for the loss of self-renewal (i.e., loss of stem cell marker expression and sphere formation capacity) but not for the induction of differentiation of GICs.

Hydrogen peroxide promotes Bmi1 protein degradation in a p38 MAPK-dependent manner

We have demonstrated earlier in this study that the ROS–p38 axis mediates hydrogen peroxide-induced loss of self-renewal and differentiation of GICs. We next wished to determine, therefore, the mechanistic link between p38 activation and Bmi1 downregulation in GICs. Notably, while conducting detailed time course analysis of Bmi1 mRNA and protein expression, we found that the mechanism of reduced Bmi1 protein expression is primarily post-transcriptional: whereas reduced protein expression of Bmi1 was apparent as early as 8 h after hydrogen peroxide treatment (Fig. 4A), the mRNA expression of Bmi1 remained unchanged even at 24 h

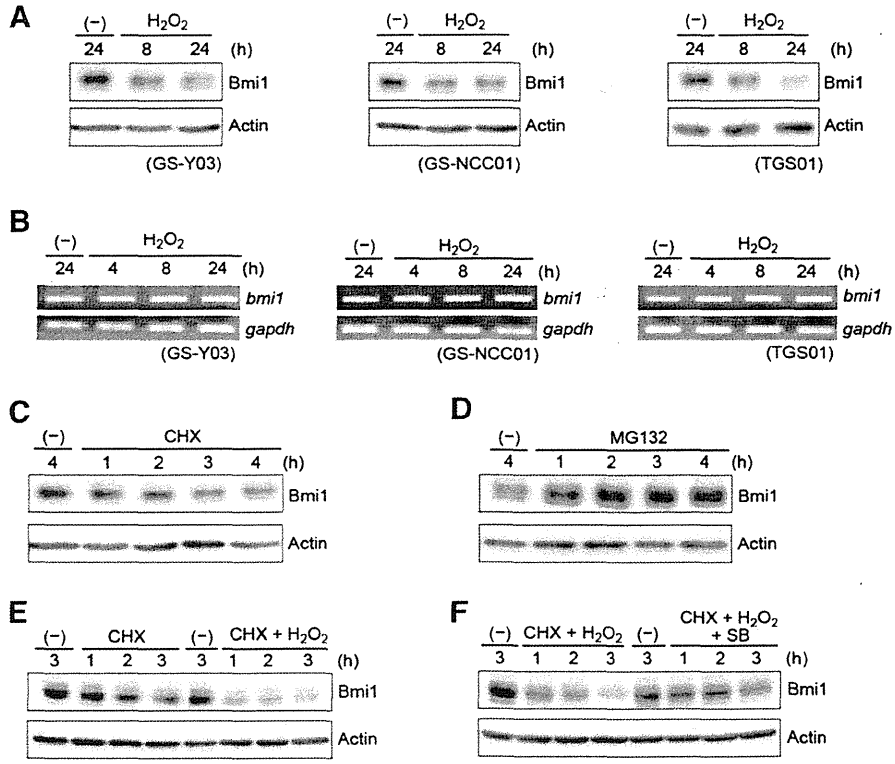

Figure 4 Hydrogen peroxide promotes Bmi1 protein degradation in a p38 MAPK-dependent manner. (A, B) The indicated GICs treated with or without H_2O_2 (100 μM) for the indicated periods were subjected to immunoblot (A) and RT-PCR (B) analyses for protein and mRNA expression of Bmi1, respectively. (C, D) GS-Y03 cells treated with or without cycloheximide (CHX, 50 μg/ml) (C) or MG132 (20 μM) (D) for the indicated periods were subjected to immunoblot analysis for Bmi1 protein expression. (E, F) GS-Y03 cells treated with the indicated combinations of cycloheximide (CHX, 50 μg/ml), H_2O_2 (100 μM), and SB203580 (SB, 10 μM) for the indicated periods were subjected to immunoblot analysis for Bmi1 protein expression. In (F), SB203580 was added to the culture medium 30 min before cycloheximide and H_2O_2.

(Fig. 4B; Fig. S8). To determine whether Bmi1 is regulated at the post-transcriptional level through proteasomal degradation as recently reported (Kim et al., 2011), we examined the time course of Bmi1 protein expression in the absence of de novo protein synthesis using cycloheximide, and also examined the effect of MG132, a proteasomal inhibitor, on Bmi1 protein expression. The results suggested that the Bmi1 protein is rapidly degraded (Fig. 4C; Fig. S9A) in the GICs and that proteasome activity may be involved in Bmi1 protein degradation (Fig. 4D; Fig. S9B). We then asked whether hydrogen peroxide promotes degradation of the Bmi1 protein and, if so, in a p38-dependent manner. Consistent with the recent report (Kim et al., 2011), hydrogen peroxide promoted Bmi1 protein degradation in a p38-dependent manner in the GICs (Figs. 4E and F; Figs. S9C and D).

Hydrogen peroxide activates FoxO3, an inducer of differentiation of GICs, in a p38 MAPK-dependent manner

Thus far, we have shown that, whereas the ROS-p38 axis mediates both loss of self-renewal and differentiation of GICs induced by hydrogen peroxide, p38-mediated degradation of Bmi1 may be responsible for the loss of self-renewal but not for the differentiation of GICs. Our results therefore give rise to the idea that there exists another molecule(s) aside from Bmi1 mediating the differentiation signal elicited by hydrogen peroxide. Intriguingly, we have recently demonstrated that, in contrast to leukemia-initiating cells of chronic myeloid leukemia which require FoxO3 for their maintenance (Naka et al., 2010), FoxO3 activation is rather required for the differentiation but not for the loss of self-renewal of stem-like GICs induced by hydrogen peroxide, which was confirmed also in the experimental condition of this study (Figs. 5A and B; Figs. S10A and B). We therefore hypothesized that FoxO3 could be the missing link between the ROS–p38 axis and differentiation. To test this idea, we investigated the role of ROS and p38 in hydrogen peroxide-induced activation of FoxO3. As reported previously, FoxO3 is expressed predominantly in the cytoplasm of untreated GICs, but hydrogen peroxide treatment caused FoxO3 activation as evidenced by its accumulation in the nucleus (Figs. 5C and D; Figs. S10C and D). However, FoxO3 activation was almost completely prevented when the GICs were treated with hydrogen peroxide in the presence of NAC (Fig. 5C; Fig. S10C), SB203580 (Fig. 5D; Fig. S10D), or siRNAs against p38 (Fig. 5E), suggesting that hydrogen peroxide activation of FoxO3 is dependent on the increase in intracellular ROS and p38 activation. Collectively, the data are in support of the idea that the

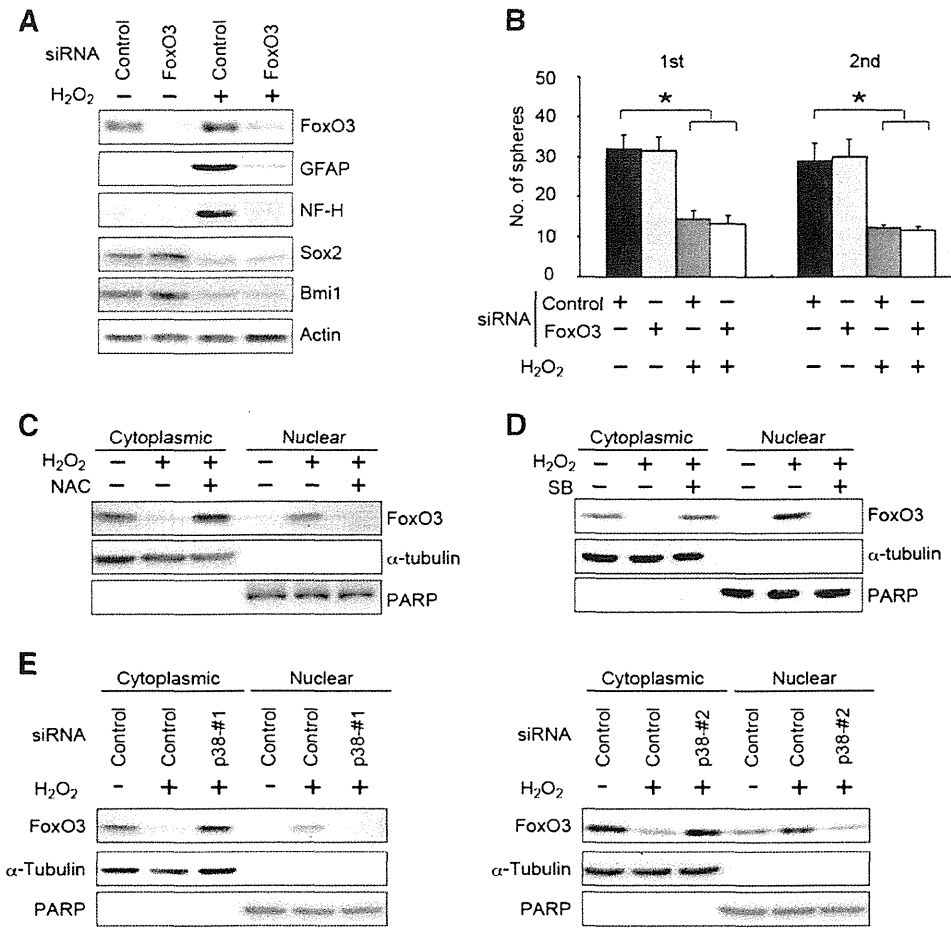

Figure 5 Hydrogen peroxide activates FoxO3, an inducer of GIC differentiation, in an intracellular ROS- and p38 MAPK-dependent manner. (A, B) GS-Y03 cells transfected with the indicated siRNAs were treated, 10 h after transfection, with or without H_2O_2 (100 μM) for 6 days. The cells were then subjected to immunoblot analysis (A) or to sphere formation assays (B). The data represent means ± SD from 3 independent experiments in (B). (C, D) GS-Y03 cells treated with or without H_2O_2 (100 μM) in the absence or presence of NAC (10 mM) (C) or SB203580 (10 μM) (D) for 3 days were subjected to subcellular fractionation followed by immunoblot analysis for FoxO3 as well as for α-tubulin (a cytoplasmic protein) and PARP (a nuclear protein). (E) GS-Y03 cells were transfected with the indicated siRNAs. After 10 h, the transfected cells were treated with or without H_2O_2 (100 μM) for 6 days and then subjected to subcellular fractionation followed by immunoblot analysis for FoxO3 as well as for α-tubulin (a cytoplasmic protein) and PARP (a nuclear protein).

hydrogen peroxide-elicited intracellular signals culminating in the loss of self-renewal and differentiation of GICs are transmitted through the ROS–p38 axis and then diverge to be mediated by Bmi1 and FoxO3, respectively (see Discussion section).

p38-dependent promotion of GIC differentiation induced by L-buthionine sulfoximine, an inhibitor of GSH biosynthesis

Having shown that the ROS–p38 axis plays a pivotal role in the loss of self-renewal and differentiation of GICs induced by exposure to exogenous ROS (i.e., hydrogen peroxide treatment), most likely through modulation of Bmi1 and FoxO3, we next wished to ask whether the ROS–p38 axis could play a role in the control of GICs in the absence of exogenously applied ROS. To this end, we treated GICs with L-buthionine sulfoximine (BSO), an inhibitor of GSH biosynthesis (Bailey, 1998; Boivin et al., 2011). Treatment of GICs with BSO caused the accumulation of intracellular ROS (Figs. 6A and B; Figs. S11A and B) as well as the phosphorylation of p38 and ATF2 (Figs. 6C and E; Figs. S11C and E). BSO also induced differentiation of the GICs, as evidenced by decreased and increased expression of stem cell and differentiation markers (Figs. 6D and E; Figs. S11D and E), respectively. Importantly, all these changes caused by BSO were prevented when the intracellular ROS were depleted by NAC (Figs. 6C and D; Figs. S11C and D) or when p38 activation was inhibited by SB203580 (Fig. 6E; Fig.

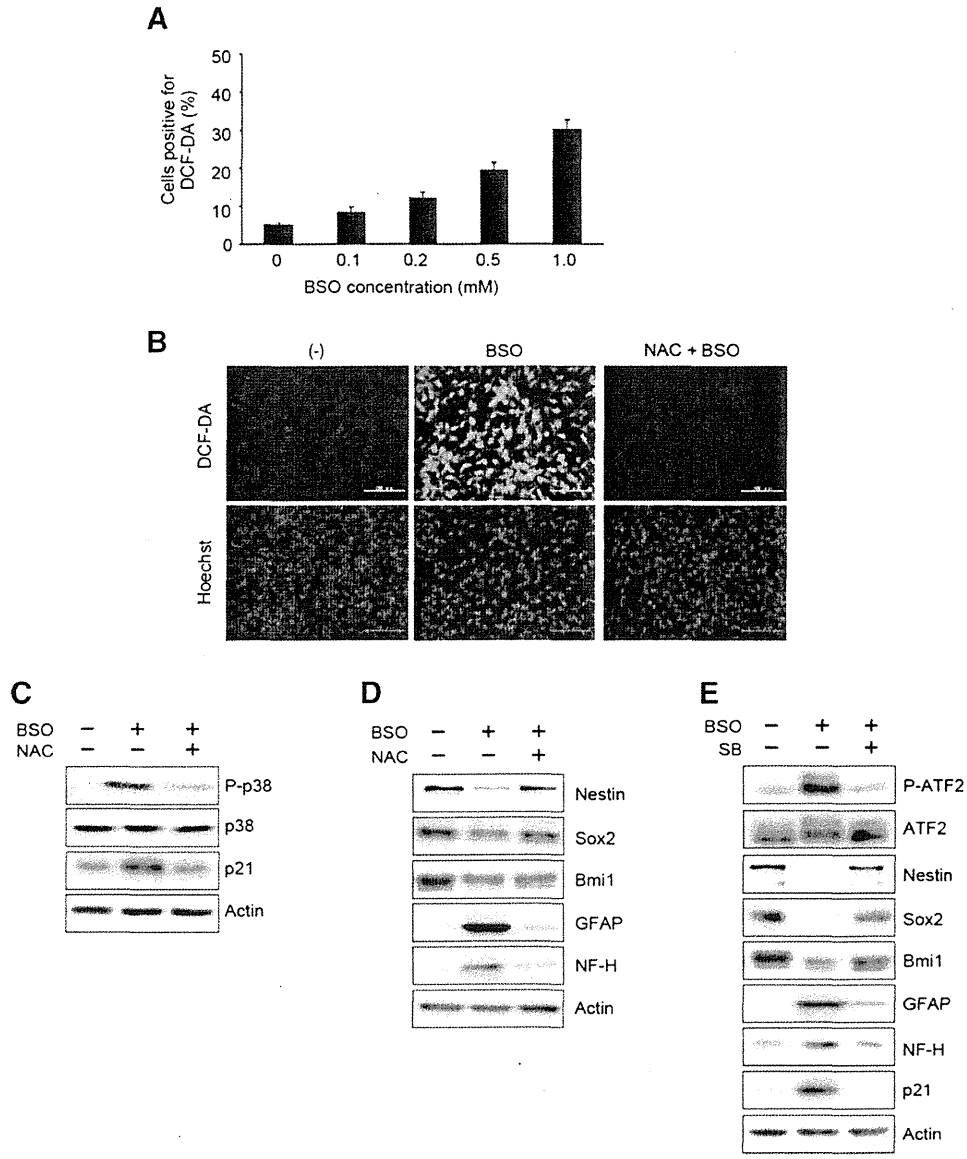

Figure 6 p38 MAPK-dependent promotion of GIC differentiation induced by L-buthionine sulfoximine (BSO), an inhibitor of GSH biosynthesis. (A) GS-Y03 cells treated with the indicated concentrations of BSO for 30 min were stained with DCF-DA and analyzed by flow cytometry. The graph shows the percentage of cells positive for DCF-DA. The data represent means ± SD from 3 independent experiments. (B) GS-Y03 cells cultured in the presence or absence of NAC (10 mM) for 30 min were further treated with BSO (1 mM) for 30 min. The cells were then stained with DCF-DA and subjected to fluorescence microscopy after nuclear staining with Hoechst 33342 (Hoechst). Identical visual fields are shown for each pair of DCF-DA and Hoechst staining. Scale bars, 100 μm. (C–E) GS-Y03 cells cultured in the absence or presence of NAC (10 mM) (C and D) or SB203580 (SB, 10 μM) (E) for 30 min were further treated with or without BSO (1 mM) for 6 days. The cells were then subjected to immunoblot analyses of the indicated proteins.

S11E). Thus, these results suggest that GICs may undergo ROS–p38 axis-dependent differentiation when the antioxidant defense mechanism is inactivated.

Pivotal role for ROS-dependent p38 MAPK activation in oxidative stress-induced loss of tumor-initiating capacity of GICs

Having demonstrated the role of the ROS–p38 axis in the control of the differentiation process of GICs, we next wished to ask whether ROS activation of p38 also plays a role in the control of tumor-initiating capacity of GICs as well as of their differentiation. As we have reported previously, treatment of GICs with hydrogen peroxide before implantation significantly extended survival of mice in the intracranial xenograft model (Fig. 7A) (Sunayama et al., 2011). We then examined the effect of the antioxidant NAC and p38 inhibitor SB203580 in the xenograft analysis. Strikingly, whereas treatment of GICs with either NAC or SB203580 alone before implantation had no discernible effect on the survival of the mice (Fig. 7B), co-treatment with NAC or SB203580 almost totally canceled